A NEW FOUR-QUADRANT INVERTER BASED ON DUAL-WINDING ISOLATED CUK CONVERTERS FOR RAILWAY AND RENEWABLE ENERGY APPLICATIONS

Saud Alotaibi[1], Ahmed Darwish[1*], Xiandong Ma[1] and Barry W. Williams[2]

[1]Lancaster University, Department of Engineering, Lancaster, United Kingdom
[2]University of Strathclyde, Electrical and Electronic Engineering Department, Glasgow, United Kingdom
**a.badawy@lancaster.ac.uk*

Keywords: POWER ELECTRONICS, CUK CONVERTER, RAILWAY APPLICATIONS, PHOTOVOLTAIC RENEWABLE ENERGY

Abstract

The paper presents a new four-quadrant converter based on dual-winding isolated Cuk converters. The proposed converter can operate as a DC/DC converter, DC/AC inverter or AC/DC rectifier. The new converter offers important merits such as losses reduction, voltage boosting, flexible output voltage range, passive element reduction and galvanic isolation with small-size high-frequency transformers. If the proposed converter output is applied to a DC motor, providing the possibility of motoring, braking and regenerative braking if required. In addition, the converter offers the possibility to generate AC voltages and currents if it is employed in renewable energy systems as a DC/AC inverter. The paper presents the description of the converter with the associated mathematical analysis. Simulation results are obtained using MATLAB/SIMULINK software while experimental results are obtained using a scaled down prototype, controlled by TMS320F28335DSP.

1 Introduction

The remarkable progress in semiconductor devices and power electronic systems allows for further reduction of power losses in railway systems [1]. DC railway systems may be preferred in the short distance train lines as they do not require on-board large transformers [2]. In these systems, the electric lines supply a DC/DC converter in the first stage to regulate the voltage input voltage. In the second stage, another converter is controls a DC motor or an inverter when employing an AC motor [2].

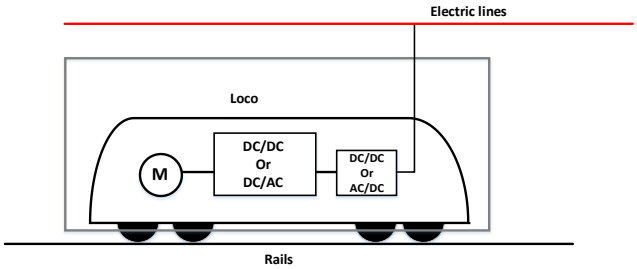

Fig. 1 A typical locomotive

In the case of AC railway systems, the power is supplied at 16.7 Hz and therefore a bulky transformer is required at this low frequency [3]. For this reason, isolated converters based on high-frequency small-size transformers can be employed in this application to provide the required galvanic isolation, voltage boosting and current shaping [4]. In this context, it is necessary to employ power electronic converters with small size, reduced power losses and low weight. The conventional voltage source inverter (VSI) and H-Bridge converter are commonly used for AC and DC motors respectively [5]. Both converters emerged originally from the conventional buck converter and therefore draw discontinuous current from the input supply. Thus, a large capacitor should be installed at the input side to filter the ripple in the input current [6]. At high voltages, this input capacitor will be an electrolytic type. Electrolytic capacitors are known to degrade reliability especially at high power [7]. The life time of an electrolytic capacitor halves for every ten degrees increase in temperature [8]. The Cuk converter has been used extensively in power systems as it provides continuous input current, requires small filtering capacitance at the input and output sides, allow for small-size isolating transformers if the pulse-width-modulation operates at high frequency, and provides a flexible range of output voltages lower or higher than the input voltage [9, 10]. The Cuk converter can operate with more than one transformer secondary winding as shown in Fig. 2. If the gate signal is the same for the output switches S_{o1} and S_{o2}, the output voltages v_{o1} and v_{o2} will be equal.

This paper presents a new DC/DC converter based on the isolated dual secondary winding Cuk converter for motor control in railway systems. The proposed converter is able to work in four-quadrant operation using two gate signals for the semiconductor switches. The proposed system can be extended to DC/AC inverters to drive AC motors in the railway applications or in renewable energy systems such as photovoltaic (PV) systems.

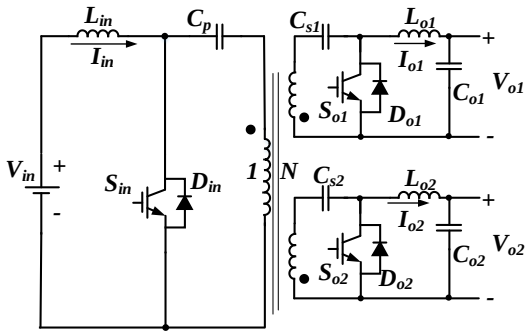

Fig. 2 Dual secondary winding Cuk converter

The remainder of this paper is arranged as follows: Section 2 describes the proposed system and mathematical modelling for the dual winding Cuk converter, Section 3 presents the modulation scheme for DC/DC converter system and MATLAB simulation results for the DC/DC converter. Section 5 presents the modulation of the DC/AC inverter and MATLAB simulations. Section 6 presents experimental results for the converter when operating as a DC/DC converter controlling a BURSA DC motor and when operating as a DC/AC inverter supplying a 1 kW, 240Vrms load.

2 Dual-winding Cuk Converter Modelling

As shown in Fig. 3 the dual secondary winding Cuk converter operates in two modes (S_{in} on and S_{in} off):

i) $0 \le t < t_{on}$

During this mode, S_{in} is ON while the output switches S_{o1} and S_{o2} are OFF. The input current I_{in} increases and the inductor L_{in} is charged while all capacitors C_p, C_{s1} and C_{s2} are discharging into the loads. The state-space representation of this mode can be expressed as:

$$\begin{bmatrix} \dot{i}_{in} \\ \dot{v}_{cp} \\ \dot{v}_{cs1} \\ \dot{v}_{cs2} \\ \dot{i}_{Lo1} \\ \dot{i}_{Lo2} \\ \dot{v}_{o1} \\ \dot{v}_{o2} \end{bmatrix} = \begin{bmatrix} 0 & 0 & 0 & 0 & 0 & 0 & 0 & 0 \\ 0 & 0 & 0 & 0 & \frac{-N}{C_p} & \frac{-N}{C_p} & 0 & 0 \\ 0 & 0 & 0 & 0 & \frac{-1}{C_{s1}} & 0 & 0 & 0 \\ 0 & 0 & 0 & 0 & \frac{-1}{C_{s2}} & 0 & 0 & 0 \\ 0 & \frac{N}{L_{o1}} & \frac{1}{L_{o1}} & 0 & 0 & 0 & \frac{-1}{L_{o1}} & 0 \\ 0 & \frac{N}{L_{o2}} & 0 & \frac{1}{L_{o2}} & 0 & 0 & 0 & \frac{-1}{L_{o2}} \\ 0 & 0 & 0 & 0 & \frac{1}{C_{o1}} & 0 & 0 & 0 \\ 0 & 0 & 0 & 0 & 0 & \frac{1}{C_{o1}} & 0 & 0 \end{bmatrix} \begin{bmatrix} i_{in} \\ v_{cp} \\ v_{cs1} \\ v_{cs2} \\ i_{Lo1} \\ i_{Lo2} \\ v_{o1} \\ v_{o2} \end{bmatrix} + \begin{bmatrix} \frac{1}{L_{in}} & 0 & 0 \\ 0 & 0 & 0 \\ 0 & 0 & 0 \\ 0 & 0 & 0 \\ 0 & 0 & 0 \\ 0 & \frac{-1}{C_{o1}} & 0 \\ 0 & \frac{-1}{C_{o2}} & 0 \end{bmatrix} \begin{bmatrix} V_{in} \\ i_{L1} \\ i_{L2} \end{bmatrix} \quad (1)$$

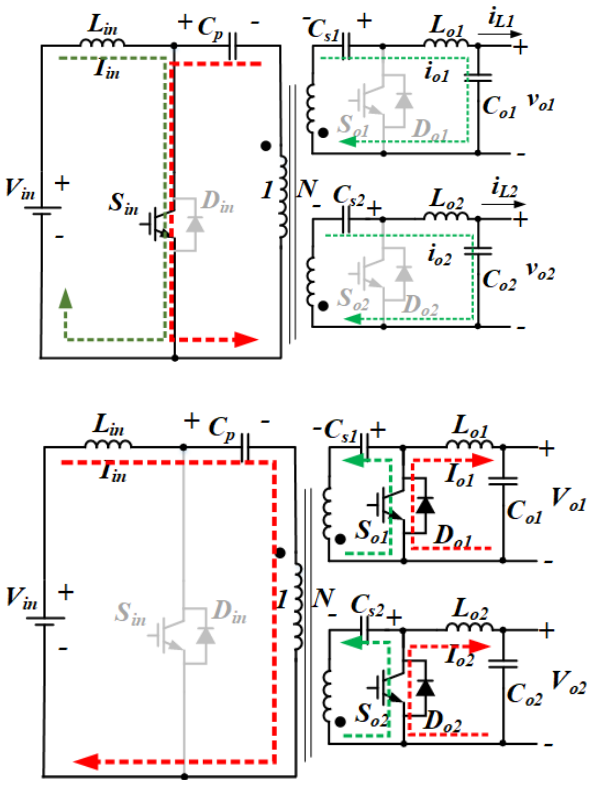

Fig. 3 Dual-winding Cuk converter Modes of Operation: (a) $0 \le t < t_{on}$ and (b) $t_{on} \le t < t_s$

ii) $t_{on} \le t < t_s$

In this mode, S_{in} is OFF while the output switches S_{o1} and S_{o2} are ON. The state-space representation of this mode can be expressed as:

$$\begin{bmatrix} \dot{i}_{in} \\ \dot{v}_{cp} \\ \dot{v}_{cs1} \\ \dot{v}_{cs2} \\ \dot{i}_{Lo1} \\ \dot{i}_{Lo2} \\ \dot{v}_{o1} \\ \dot{v}_{o2} \end{bmatrix} = \begin{bmatrix} 0 & \frac{-1}{L_{in}} & \frac{-1}{2NL_{in}} & \frac{-1}{2NL_{in}} & 0 & 0 & 0 & 0 \\ \frac{1}{C_p} & 0 & 0 & 0 & 0 & 0 & 0 & 0 \\ \frac{1}{NC_{s1}} & 0 & 0 & 0 & 0 & 0 & 0 & 0 \\ \frac{1}{NC_{s1}} & 0 & 0 & 0 & 0 & 0 & 0 & 0 \\ 0 & 0 & 0 & 0 & 0 & 0 & \frac{-1}{L_{o1}} & 0 \\ 0 & 0 & 0 & 0 & 0 & 0 & 0 & \frac{-1}{L_{o2}} \\ 0 & 0 & 0 & 0 & \frac{1}{C_{o1}} & 0 & 0 & 0 \\ 0 & 0 & 0 & 0 & 0 & \frac{1}{C_{o1}} & 0 & 0 \end{bmatrix} \begin{bmatrix} i_{in} \\ v_{cp} \\ v_{cs1} \\ v_{cs2} \\ i_{Lo1} \\ i_{Lo2} \\ v_{o1} \\ v_{o2} \end{bmatrix} + 0 + \begin{bmatrix} \frac{1}{L_{in}} & 0 & 0 \\ 0 & 0 & 0 \\ 0 & 0 & 0 \\ 0 & 0 & 0 \\ 0 & 0 & 0 \\ 0 & \frac{-1}{C_{o1}} & 0 \\ 0 & \frac{-1}{C_{o2}} & 0 \end{bmatrix} \begin{bmatrix} V_{in} \\ i_{L1} \\ i_{L2} \end{bmatrix} \quad (2)$$

Thus, averaging the two state-space representation along the two modes during the switching time t_s yields:

$$\begin{bmatrix} \dot{i}_{in} \\ \dot{v}_{cp} \\ \dot{v}_{cs1} \\ \dot{v}_{cs2} \\ \dot{i}_{Lo1} \\ \dot{i}_{Lo2} \\ \dot{v}_{o1} \\ \dot{v}_{o2} \end{bmatrix} = \begin{bmatrix} 0 & \frac{D-1}{L_{in}} & \frac{D-1}{2NL_{in}} & \frac{D-1}{2NL_{in}} & 0 & 0 & 0 & 0 \\ \frac{D-1}{C_p} & 0 & 0 & 0 & \frac{-ND}{C_p} & \frac{-ND}{C_p} & 0 & 0 \\ \frac{1-D}{NC_{s1}} & 0 & 0 & 0 & \frac{-D}{C_{s1}} & 0 & 0 & 0 \\ \frac{1-D}{NC_{s2}} & 0 & 0 & 0 & \frac{-D}{C_{s2}} & 0 & 0 & 0 \\ 0 & \frac{ND}{L_{o1}} & \frac{D}{L_{o1}} & 0 & 0 & 0 & \frac{-1}{L_{o1}} & 0 \\ 0 & \frac{ND}{L_{o2}} & 0 & \frac{D}{L_{o2}} & 0 & 0 & 0 & \frac{-1}{L_{o2}} \\ 0 & 0 & 0 & 0 & \frac{1}{C_{o1}} & 0 & 0 & 0 \\ 0 & 0 & 0 & 0 & 0 & \frac{1}{C_{o1}} & 0 & 0 \end{bmatrix} \begin{bmatrix} i_{in} \\ v_{cp} \\ v_{cs1} \\ v_{cs2} \\ i_{Lo1} \\ i_{Lo2} \\ v_{o1} \\ v_{o2} \end{bmatrix} + \begin{bmatrix} \frac{1}{L_{in}} & 0 & 0 \\ 0 & 0 & 0 \\ 0 & 0 & 0 \\ 0 & 0 & 0 \\ 0 & 0 & 0 \\ 0 & 0 & 0 \\ 0 & \frac{-1}{C_{o1}} & 0 \\ 0 & \frac{-1}{C_{o2}} & 0 \end{bmatrix} \begin{bmatrix} V_{in} \\ i_{L1} \\ i_{L2} \end{bmatrix} \quad (3)$$

where $D = t_{on}/t_s$ and $t_s = t_{on} + t_{off}$ (continuous conduction mode)

The voltage and current conversion ratios of the converter in the steady state are:

$$v_o = \frac{ND}{1-D} V_{in} \quad (4a)$$

$$i_{in} = \frac{ND}{1-D}(i_{o1} + i_{o2}) \quad (4b)$$

3 System Description

The proposed system is shown in Fig. 4 where the two windings of converter *A* are connected to the load motor to control it in the forward direction while the two windings of converter *B* are connected to the load motor to control it in the reverse direction. If all the windings are identical and the passive element values are equal in both converters *A* and *B*, the system will operate using four gate signals. Any gate signal of the converter is generated by comparing the duty-cycle ratio to the carrier signal as shown in Fig. 5.

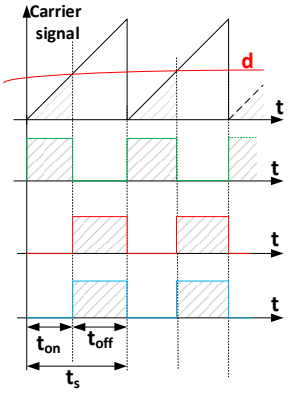

Fig. 5. Modulation principle of the converter

The proposed system can operate in DC/DC or DC/AC modes. The differential voltage seen by the load v_m is

$$v_m = v_{o1\_B} - v_{o1\_A} = v_{o2\_B} - v_{o2\_A} \quad (5)$$

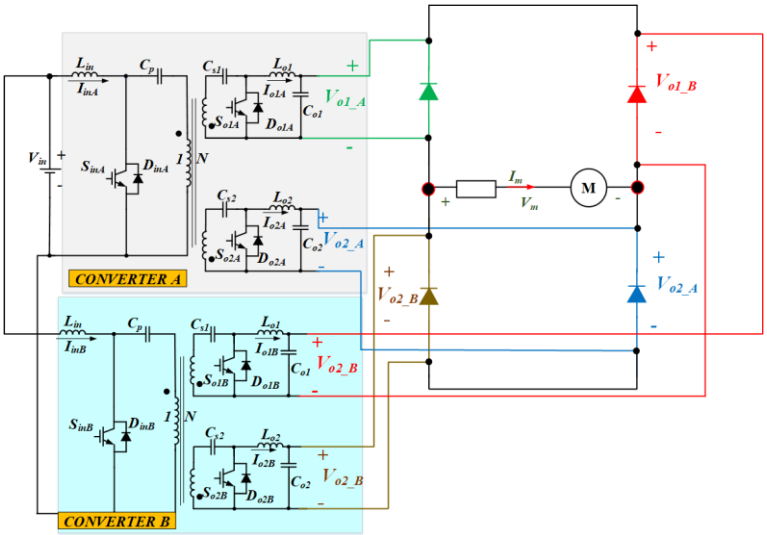

Fig. 4 Proposed System

If d_A and d_B are the duty-cycle ratios of converters *A* and *B* respectively, the load voltage is expressed as:

$$v_m = \left(\frac{d_B}{1-d_B} - \frac{d_A}{1-d_A}\right) N V_{in} \qquad (6)$$

4 DC/DC operation

In DC/DC operation, the output voltage v_m is positive when the windings of converter *B* have finite values while converter *A* generates zero voltages. Similarly, v_m is negative when converter *A* has finite voltage values while converter *B* generates zero voltages. MATLAB simulation results will be used in this section to show the performance of the proposed system when using the parameters shown in Table 1.

Fig. 6 shows the proposed system operating the motor in the forward direction (Quadrant 1). The motor starts from zero speed and is required to reach the maximum speed in 2s. The motor's torque is shown in Fig. 6b. Converter winding voltages are shown in Fig. 6c and d. The armature current is shown in Fig. 6e while the total input current of the system is shown in Fig. 6f.

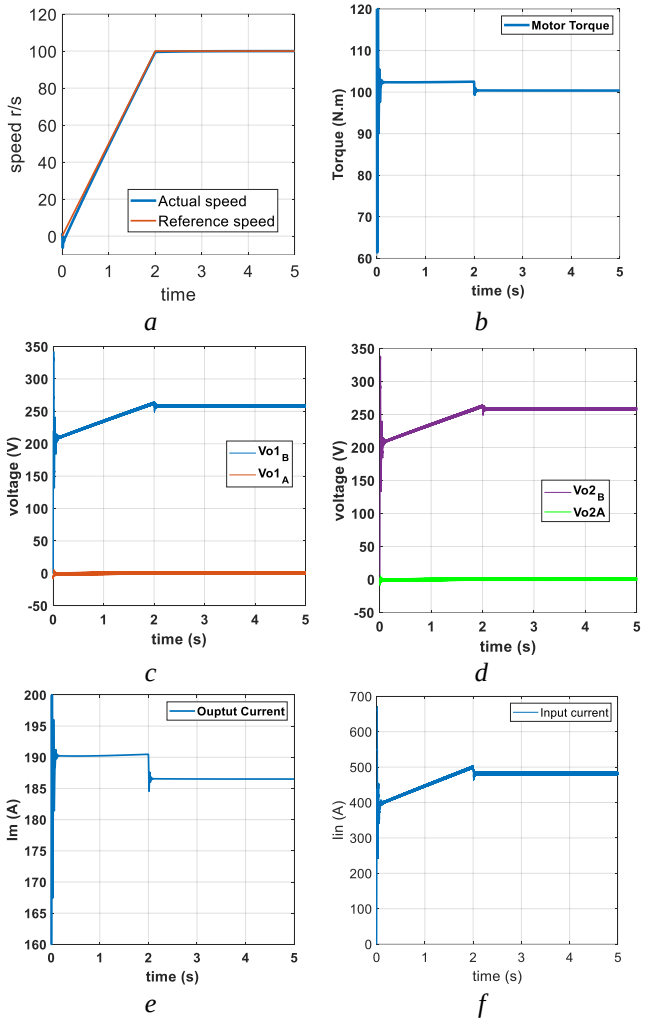

Fig. 6 Motoring action: (a) motor speed, (b) motor torque, (c) and (d) converter voltages, (e) output current, and (f) input current

Table 1 Simulation Parameters

Symb	Parameter	Value
L_{in}	Input Inductance	2 mH
C_p	Primary side capacitance	10 µF
C_s	Secondary side capacitance	10 µF
L_o	Output Inductance	1 mH
N	Transformer Turns ratio	2
f_s	Switching (sampling)	50 kHz
L_o	Output capacitance	1 µF
V_{in}	Nominal input voltage	100 V
P_m	Motor peak power	10 hp
RPM	Motor rated rpm	1000 rpm
L_a	Armature inductance	1.2 mH
R_a	Armature Resistance	1 Ω
J	Motor Inertia	0.0425 kg.m^2
vf	Viscous friction	0.00346 N.m.s

Fig. 7 shows the same machine in the braking mode (Quadrant 4) when the motor is required to brake at time t = 5s as shown in Fig. 7a.

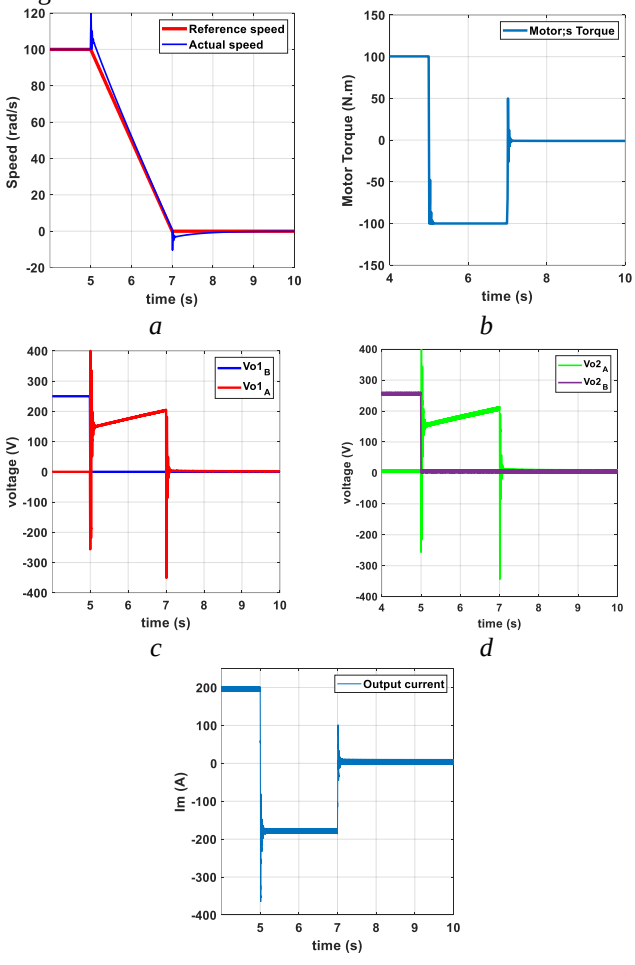

Fig. 7 Motor Braking: (a) motor speed, (b) motor torque, (c) and (d) converter voltages, and (e) output current

The motor reversed its armature voltage v_m and to reverse the electromagnetic torque as shown in Fig. 7b. The motor's voltage is reversed by means of changing winding voltages as shown in Fig. 7c and d.

5 Modular DC/AC operation

The proposed topology can be employed as a modular DC/AC inverter to provide high voltage boosting if the windings generate as shown in Fig. 8. The voltages of the converters can be calculated as:

$$v_{oA} = \begin{cases} V_m \sin \omega t & 0 \geq \omega t \geq \pi \\ 0 & \pi > \omega t \geq 2\pi \end{cases}$$

$$v_{oB} = \begin{cases} 0 & 0 \geq \omega t \geq \pi \\ V_m \sin(\omega t + \pi) & \pi > \omega t \geq 2\pi \end{cases} \quad (7)$$

The load voltage can be doubled:

$$v_m = 2V_m \sin(\omega t + \pi) \quad (8)$$

The duty cycle ratios are:

$$d_A = \frac{v_{oA}}{v_{oA} + NV_{in}} \quad (9a)$$

$$d_B = \frac{v_{oB}}{v_{oB} + NV_{in}} \quad (9b)$$

The proposed inverter can provide a higher level of voltage boosting if the secondary sides of the Cuk converter have more than two windings. Fig. 9 shows the simulation results when the proposed system is used to generate 800V across a 20 Ω load. Fig. 9a and 9b show the winding voltages and duty-cycle ratios to generate these voltages. The total input current supplied from the 100V supply voltage is shown in Fig. 9d with the load current in Fig. 9c.

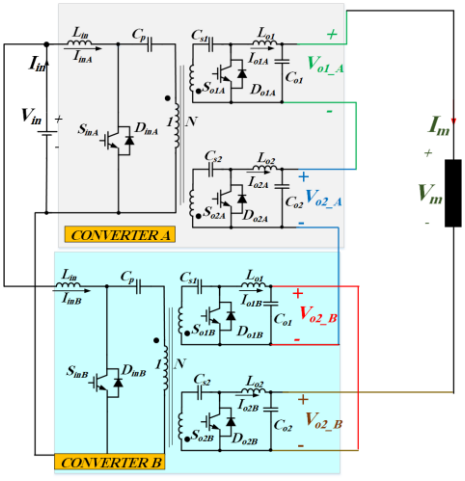

Fig. 8 Modular DC/AC inverter

6 Experimentation

Experimental results provide proof of concept for both DC/DC and DC/AC operation. The experimental results for the latter are shown in Fig. 10a. To test the DC/DC operation, BRUSA MD-609 motors are used with the converters as shown in Fig. 10b.

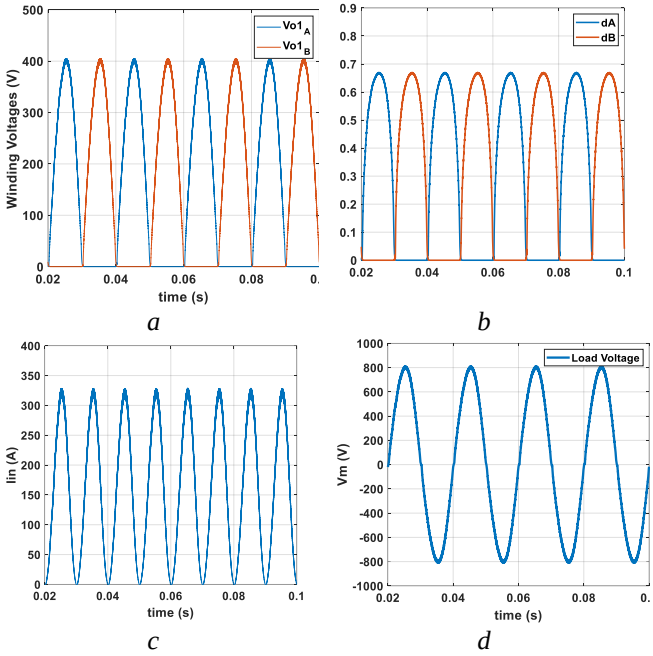

Fig. 9 Modular DC/AC Inverter: (a) winding voltages V_{o1_A} and V_{o1_B}, (b) duty-cycle ratio, (c) input current, and (d) load voltage

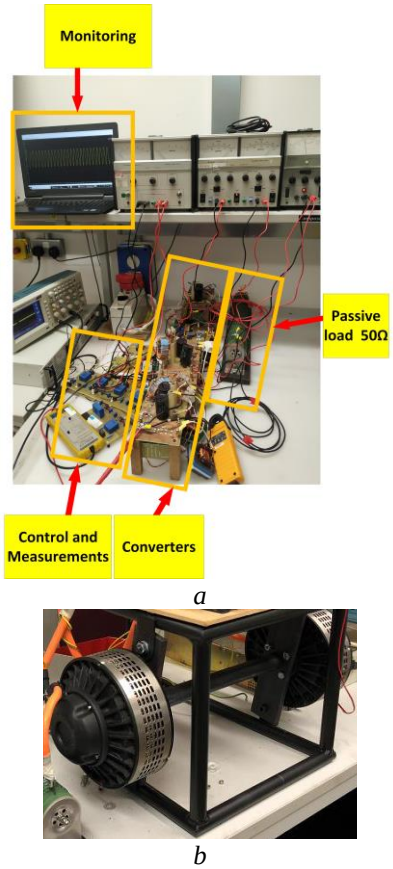

Fig. 10 Experimental Setup: (a) converters and (b) BRUSA MD-609 Motors

Fig. 11a shows the voltages of the converter when the motor is required to start from stand still until reaching 1500 rpm in 5s when the converters are supplied from 120 VDC battery. The battery current is shown in Fig. 11b. To test DC/AC inverter operation, a 50V DC power supply is connected to the converters as shown in Fig. 8 and the system is controlled to generate 240 Vrms ac voltage at 50 Hz across the passive load. The load voltage is shown in Fig. 12a while the input current is shown in Fig. 12b.

7 Conclusion

The paper presented a new energy conversion system based on dual secondary winding isolated Cuk converters. If the proposed system is employed as a DC/DC converter, it can control DC motors in a railway network and offers the capability of regenerative braking and four-quadrant operation. The proposed converter is capable of operating as a modular DC/AC inverter which is important in renewable energy system, energy storage, and grid-connected applications. The proposed topology is isolated with small-size high-frequency nano-crystalline cores. The proposed system employs small passive element components and therefore reduces the voltage/current ripple, weight and power losses. As the converters are current sourced at the input and output sides, small plastic or film capacitors can be used which can reduce the system size significantly.

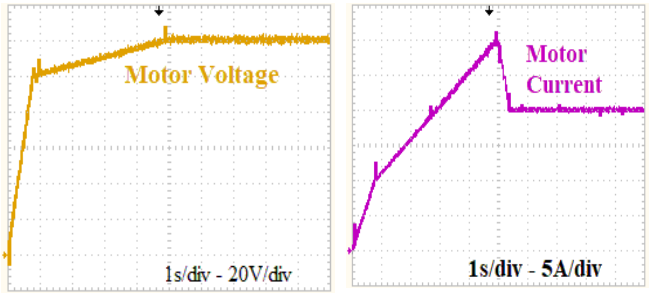

a *b*

Fig. 11 BRUSA MD-609 Motor: (a) voltage and (b) current

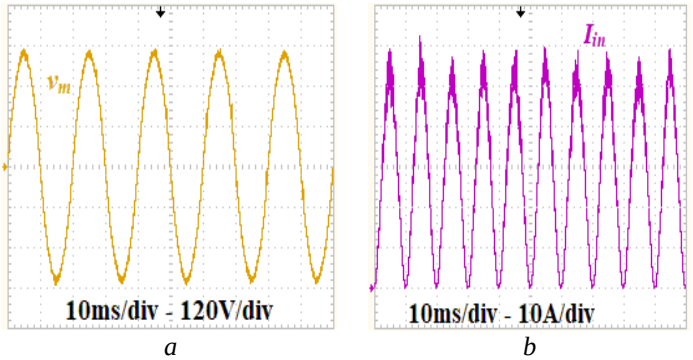

a *b*

Fig. 12 Experimental results of the proposed system in Fig. 8: (a) load voltage v_m and (b) input current I_{in}

8 References

[1] Shigeeda, H., Morimoto, H., Ito, K., Fuji., T, and Morishima. N.: 'Feeding-loss Reduction by Higher-voltage DC Railway Feeding System with DC-to-DC Converter' 2018 International Power Electronics Conference (IPEC-Niigata 2018 -ECCE Asia), Niigata, 2018, pp. 2540-2546.

[2] Heising. C., Bartelt, R., Staudt, V., and Steimel, A.: 'Single-phase 50-kW 16.7-Hz four-quadrant line-side converter for railway traction application' 2008 13th International Power Electronics and Motion Control Conference, Poznan, 2008, pp. 521-527.

[3] Steimel, A: 'Electric Traction – Motive Power and Energy Supply', Oldenbourg – Velrag, Munchen 2008

[4] Darwish, A., Massoud, A.M., Holliday, D., Ahmed, S., and Williams, B.W.: 'Single-Stage three-phase differential-mode buck-boost inverters with continuous input current for PV Applications,' in IEEE Transactions on Power Electronics, vol. 31, no. 12, pp. 8218-8236, Dec. 2016.

[5] Kjaer, S. B., Pederson, J. K., and Blaabjerg, F. 'A review of single-phase grid-connected inverters for photovoltaic modules, ' IEEE Trans. Ind. Appl., vol. 41, no. 5, pp. 1292-1306, Sep/Oct. 2005.

[6] Darwish Badawy, A.: 'Current source dc-dc and dc-ac converters with continuous energy flow, ' Degree of Doctor of Philosophy, Department of Electronics and Electrical Engineering, University of Strathclyde, Glasgow, 2015.

[7] Williams, B. W.: 'Generation and analysis of canonical switching Cell DC to-DC converters, ' IEEE Trans. Ind. Electron., vol. 61, no. 1, pp. 329–346, Jan. 2013.

[8] Knight, J. Shirsavar, S. and Holderbaum, W.: 'An improved reliability cuk based solar inverter with sliding mode control, ' in IEEE Transactions on Power Electronics, vol. 21, no. 4, pp. 1107-1115, July 2006.

[9] Darwish, A. Massoud, A. Holliday, D. Ahmed, S. and Williams, B. W.: 'Generation, performance evaluation and control design of single-phase differential-mode buck-boost current-source inverters, ' in IET Renewable Power Generation, vol. 10, no. 7, pp. 916-927, 7 2016.

[10] Darwish, A. Elserougi, A. Abdel-Khalik, A. , Massoud, A. Holliday, D. and Williams, B.W.: 'A single-stage three-phase DC/AC inverter based on Cuk converter for PV application, ' in GCC Conference and Exhibition (GCC), 2013 7th IEEE, 2013, pp. 384–389